

## Article

# Polarization Diffraction Gratings in PAZO Polymer Thin Films Recorded with Digital Polarization Holography: Polarization Properties and Surface Relief Formation

Nataliya Berberova-Buhova <sup>1,2,\*</sup>, Lian Nedelchev <sup>1,2,\*</sup> , Georgi Mateev <sup>1,2</sup>, Ludmila Nikolova <sup>1</sup>, Elena Stoykova <sup>1</sup>, Branimir Ivanov <sup>1</sup>, Velichka Strijkova <sup>1</sup> , Keehoon Hong <sup>3</sup>  and Dimana Nazarova <sup>1,2</sup> 

<sup>1</sup> Institute of Optical Materials and Technologies, Bulgarian Academy of Sciences, 1113 Sofia, Bulgaria; georgi@iomt.bas.bg (G.M.); lnikolova@iomt.bas.bg (L.N.); estoykova@iomt.bas.bg (E.S.); branimirivanov@iomt.bas.bg (B.I.); vily@iomt.bas.bg (V.S.); dimana@iomt.bas.bg (D.N.)

<sup>2</sup> Department of Physics, University of Chemical Technology and Metallurgy, 8 St. Kliment Ohridski Blvd, 1756 Sofia, Bulgaria

<sup>3</sup> Electronics and Telecommunications Research Institute, 218 Gajeong-ro, Yuseong-gu, Daejeon 34129, Republic of Korea; khong@etri.re.kr

\* Correspondence: nberberova@iomt.bas.bg (N.B.-B.); lian@iomt.bas.bg (L.N.)

**Abstract:** In this work, we study the polarization properties of diffraction gratings recorded in thin films of the azopolymer PAZO (poly[1-[4-(3-carboxy-4-hydroxyphenylazo)benzene sulfonamido]-1,2-ethanediyl, sodium salt]) using digital polarization holography. Using two quarter-wave plates, the phase retardation of each pixel of the SLM is converted into the azimuth rotation of linearly polarized light. When recording from the azopolymer side of the sample, significant surface relief amplitude is observed with atomic force microscopy. In contrast, recording from the substrate side of the sample allows the reduction of the surface relief modulation and the obtaining of polarization gratings with characteristics close to an ideal grating, recorded with two orthogonal circular polarizations. This can be achieved even with a four-pixel period of grating, as demonstrated by our results.



**Citation:** Berberova-Buhova, N.; Nedelchev, L.; Mateev, G.; Nikolova, L.; Stoykova, E.; Ivanov, B.; Strijkova, V.; Hong, K.; Nazarova, D.

Polarization Diffraction Gratings in PAZO Polymer Thin Films Recorded with Digital Polarization Holography: Polarization Properties and Surface Relief Formation. *Photonics* **2024**, *11*, 425. <https://doi.org/10.3390/photronics11050425>

Received: 20 March 2024

Revised: 30 April 2024

Accepted: 1 May 2024

Published: 3 May 2024



**Copyright:** © 2024 by the authors. Licensee MDPI, Basel, Switzerland. This article is an open access article distributed under the terms and conditions of the Creative Commons Attribution (CC BY) license (<https://creativecommons.org/licenses/by/4.0/>).

**Keywords:** digital polarization holography; polarization holographic grating; azopolymer PAZO; spatial light modulator; AFM; surface relief grating

## 1. Introduction

Holography is a method used to record the wavefront transmitted or reflected by an object (object wave) by means of a second reference wave. Using the principle of interference, information about both the amplitude and the phase of the object wave is recorded, and the medium containing this information is called a “hologram”. After the invention of holography by Gabor in 1948 [1], many scientists had a significant impact on making holography a practical technology with a broad range of applications [2–4].

Most of the holographic techniques use intensity-sensitive materials (encoding only the amplitude and phase in the hologram), and, in this case, the polarization is ignored. A complete description of the wavefront, however, requires the inclusion of the polarization vector. Moreover, the polarization of light is an important characteristic, revealing the structural information of an object [5,6]. In 1956, Pancharatnam [7] considered various cases of interference of two coherent light waves with different states of polarization. Lohmann, in 1965, first proposed a method to record the polarization state of light with two orthogonally polarized reference beams [8]. The inclusion of polarization in holography has led to the development of polarization holography [9–12]. The recording material is of key importance in this case, and it has to be photoanisotropic with a high value of the photoinduced birefringence. Therefore, polarization holography employs two waves with different polarizations to record the polarization states of a polarization-sensitive photoanisotropic material [13].

In recent decades, there has been increasing scientific interest in polarization-sensitive photoanisotropic materials, due to their unique applications in polarization holography, and in photonics, as a media for the reversible optical storage of information and polarization multiplexing [14,15], for creating polarization-selective optical elements [16–18], for structures with surface modulation with high spatial frequency [19,20], to create optical switches [21,22], and more. Azobenzene-containing materials are commonly used organic materials for polarization holographic recording due to the high values of photoinduced anisotropy upon illumination with polarized light [10]. The polarization state-recording mechanism is explained through the process of selective trans-cis-trans isomerization and the subsequent reorientation of the trans azobenzene in a direction perpendicular to the electric vector of the recording linearly polarized light [10]. Natansohn and Rochon explain the mechanism of photoinduced motion in azopolymers through three types of motion—at the molecular, nanoscale, and macroscopic levels [23]. Simultaneously, with the formation of anisotropic grating in the volume of the azopolymer, a surface relief grating (SRG) is also created. This was first observed by Rochon et al. [24] and by Kim et al. [25]. Later, Holme et al. [26] reported the recording of large amplitude surface relief gratings in azopolymers. Over the years, this phenomenon has been studied by many groups [23,27–29]. The SRGs are of great interest because of their numerous applications in photonics, biophysics, and other fields [30–34].

A widely investigated azopolymer is poly[1-[4-(3-carboxy-4-hydroxyphenylazo)benzene sulfonamido]-1,2-ethanediyl, sodium salt], commonly denoted as PAZO, which is commercially available. PAZO is often the preferred material for polarization holography by many research groups, due to the high values of the photoinduced birefringence and large amplitude of the surface relief gratings [18,20,35–40]. Another important advantage of the azopolymer PAZO is that it is water soluble, thus toxic organic solvents, which are usually required for the film deposition of other azopolymers, can be avoided. These properties of PAZO allow for the easy preparation of photoanisotropic nanocomposite materials with enhanced photoinduced birefringence [34] via doping the azopolymer matrix of PAZO with nanoparticles of various chemical compositions, sizes, and shapes—silver and gold nanoparticles [29,39], goethite nanorods [20], biologically active metal complexes [40], etc.

Initially, holograms were recorded on photosensitive material, but that required time-consuming processing, including chemical treatment and mechanical focusing for the image reconstruction. In 1960, Goodman proposed the electronic recording of holograms followed by digital processing to restore the image, and this marks the beginning of digital holography [3]. Later, with the advances of technology, digitization provided new opportunities for the development of computer technology, optoelectronics, and nanotechnology. Digital holography [3,4,41–44] is a technique in which a digital hologram that contains an object wavefront is recorded in a fraction of a second directly with a CCD camera, and by using a numeric algorithm, quantitative phase images of the object are reconstructed [45]. Digital holography is widely used in the field of microscopy [42,46], quantitative phase imaging (QPI) [47,48], multiple image encryption [49,50], object recognition [51,52], and holographic 3D imaging [53]. Modern digital holographic schemes also benefit from the technological progress and employ advanced optical components such as spatial light modulators (SLMs). These devices replace the object and allow the creation of an object wave with the desired parameters. SLMs are most commonly liquid crystal devices, where the rotation of the liquid crystal molecules with respect to the supplied voltage (gray level) provides the necessary phase modulation of the corresponding pixel [54,55]. SLM is used as a dynamic (programmable) device and has wide applications [54], such as optical tweezers [56], beam shaping [57], coded aperture [58], etc.

Digital holography can be generalized to record and reconstruct the full wavefront of light—amplitude, phase, and polarization [11,59,60]. This gave rise to digital polarization holography (DPH), made possible by recording and restoring the polarization state of light [61].

Despite the intense efforts of scientists in this field, there is still a demand for the improvement of digital holography, especially for obtaining high-accuracy full-field reproduction, as well as 3D measurements of surfaces and shapes with diffractive optical elements (DOEs). DOEs are complex optical components capable of modulating light in a complex manner through the phenomenon of diffraction. Most of the known studies [62,63] regarding DOE fabrication provide good quality, but do not guarantee high diffraction efficiency or a larger modulation of the surface. In contrast, polarization holographic recording with different (or orthogonal) polarization states of the recording beams leads to an increase in the diffraction efficiency of DOEs and to a larger (deeper) photoinduced surface relief [64]. Digital polarization holographic recording with SLM allows us to spatially control the phase of the light field, thus allowing us to obtain 4G optical elements such as vector vortex waveplates [65,66], lenses [67], and other advanced geometrical phase optical elements [61].

Due to the great interest in these optical elements in recent years, many research groups are proposing different schemes for digitally recording polarization holograms (or polarization-selective diffractive optical elements) [61,68,69]. The diffraction efficiency of the recorded DOE is also monitored as an important parameter. Various applications are outlined, including the fabrication of microstructures on the surface of the optical elements. However, to the best of our knowledge, no detailed studies of the polarization properties of polarization-selective DOEs, as recorded with by DPH, have been published so far.

In this paper, we study SLM-generated polarization gratings recorded on thin film samples of the azopolymer PAZO. The main focus in our research is the investigation of the polarization properties of the polarization holographic gratings recorded in this way, evaluating the possibilities of the method for recording polarization diffraction optical elements. Two cases are considered and compared as follows: (a) recording from the substrate side of the sample, when the SRG formation is suppressed and the polarization properties are mainly determined by the volume anisotropic grating, and (b) recording from the azopolymer film side, when significant surface relief modulation is observed.

## 2. Materials and Methods

### 2.1. Samples Preparation

In the present study, we use the azopolymer poly[1-[4-(3-carboxy-4-hydroxyphenylazo) benzenesulfonamido]-1,2-ethanediyl, sodium salt], or, put shortly, PAZO, which is commercially available (Prod. #346411, Sigma Aldrich, Burlington, MA, USA). Its chemical structure and absorbance spectrum are presented in our earlier work [33]. The thin film samples were prepared by dissolving the azopolymer PAZO in methanol, and then spin-coating the solution with a concentration 100 mg/mL on cleaned and polished glass substrates (BK7) at 1000 rpm for 30 s. The thickness of the azopolymer layers is approximately  $1800 \pm 20$  nm, as measured by the F20 Optical Thin-Film Analyzer (Filmetrics, San Diego, CA, USA).

### 2.2. Optical Scheme for Digital Polarization Holographic Recording

The holographic recording of diffractive optical elements on polarization-sensitive photoanisotropic materials such as PAZO requires a coherent light beam with a wavelength within the absorption band of the azopolymer. The optical scheme used in our experiments is shown in Figure 1. The light source is a He-Cd gas laser (IK4171I G, Kimmon Koha, Tokyo, Japan) with a wavelength of 442 nm. It was selected because of its high coherence and also because its wavelength allows us to achieve the highest photoinduced birefringence in the azopolymer PAZO, as shown by our previous research [20]. The half-wave plate provides the strictly vertical linear polarization of the beam and the collimator—a spatially filtered collimated beam with uniform intensity. The linearly polarized beam is then converted to a circularly polarized beam via the quarter-wave plate (QWP1), oriented at  $+45^\circ$  with respect to the polarization direction of the incident beam. Then, the beam is reflected by a reflective high-resolution phase only spatial light modulator (LETO 3 SLM, Holoeye, Berlin, Germany), with  $1920 \times 1080$  pixels, a pixel pitch of  $6.4 \mu\text{m}$ , and a fill factor of 93%. The

active area of the SLM is  $12.29 \times 6.91$  mm, and each pixel can be addressed with 256 phase levels. The angle between the incoming and reflected beams is less than  $10^\circ$ . A periodic structure with a 4-pixel period is set on the SLM. The reflected beam is then converted into a linearly polarized beam using a second quarter-wave plate, QWP2 (its axis is set at  $-45^\circ$  with respect to the polarization direction of the input laser beam). As a result, each 4-pixel phase structure on the SLM is transformed into the light field with the periodic modulation of the azimuth, namely  $0^\circ, 45^\circ, 90^\circ,$  and  $135^\circ$ , in the consecutive horizontal pixels, as illustrated in Figure 1.

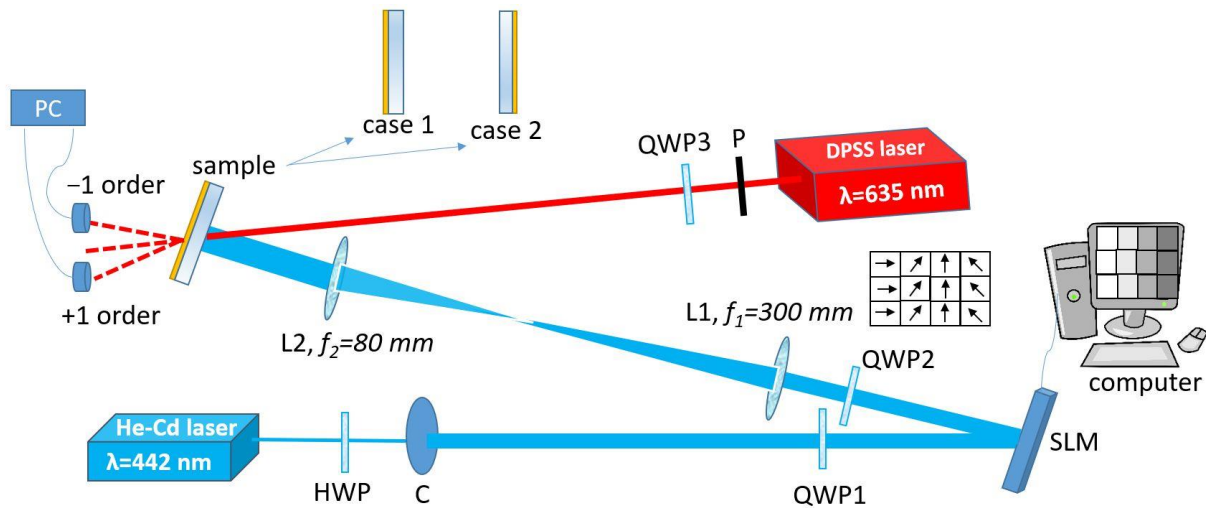


**Figure 1.** Optical setup for digital polarization holography. HWP—half-wave plate, C—collimator, QWP1 and QWP2—achromatic quarter-wave plates, QWP3—quarter-wave plate for 635 nm, SLM—spatial light modulator, L1 and L2—lenses, P—polarizer.

The lens system L1-L2 in the setup is used to image the light reflected by the SLM onto the sample carrying the photoanisotropic thin film, providing the  $f_2/f_1$  reduction in size (in our case 3.75:1) of the projected image in comparison with the SLM dimensions. Thus, the exposure area is  $3.28 \text{ mm} \times 1.84 \text{ mm}$ , or  $6.04 \text{ mm}^2$ . The power of the recording beam on the sample surface is 15 mW, hence, its intensity is about  $250 \text{ mW/cm}^2$ .

The recording is performed either through the substrate side (case 1 in Figure 1), or from the azopolymer film side of the sample (case 2). As shown by our earlier studies [18,33], in case 1, the intensity of the recording beam is significantly reduced before reaching the free surface of the azopolymer film (due to the absorbance within the film itself), and this allows us to suppress the formation of the surface relief grating. In contrast, in case 2, the intensity of the recording beam is maximal on the free surface of the azopolymer layer, and this results in high amplitude surface relief grating.

The diffraction efficiency (DE), defined as the ratio of the intensity of the desired diffracted beam and the intensity of the incidence beam, is measured in real time during the recording of the polarization holographic gratings (PHGs), simultaneously in both  $\pm 1$  diffracted orders using two computer-operated power meters (PM100D, Thorlabs, Newton, NJ, USA). For the determination of the DE, we use a probe laser beam with circular polarization (controlled via polarizer and quarter-wave plate) and a wavelength of 635 nm from a DPSS laser.

### 2.3. Optical Setup for Polarization Properties Analysis

To determine the polarization properties of the recorded polarization grating, we employ the experimental setup shown in Figure 2. It allows us to set any desired value of the azimuth or of the ellipticity of the probe beam. A similar optical scheme was employed in our recent work [33]. We use a linearly polarized probe beam from a He-Ne laser at

633 nm, and, with a half-wave plate and a quarter-wave plate, we vary the polarization of the input beam and monitor the polarization state of the light diffracted in the  $\pm 1$  orders.

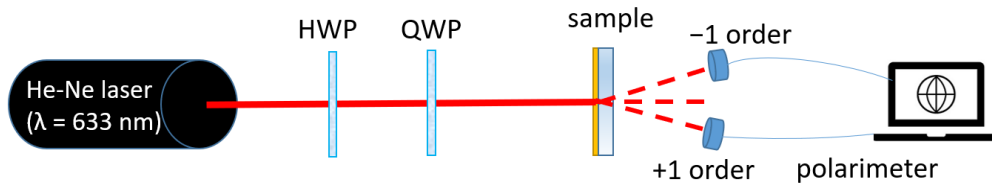


**Figure 2.** Setup for the investigation of the polarization properties of the gratings. HWP—half-wave plate, QWP—quarter-wave plate.

The measurements were performed with the input angle of ellipticity varying from  $-45^\circ$  (LCP) to  $+45^\circ$  (RCP) with a step of  $5^\circ$ . The azimuth was kept constant at  $90^\circ$  (vertical). The polarization state of the output light was determined using a PAX5710 polarimeter (Thorlabs, Newton, NJ, USA) that allowed the real-time measurement of ellipticity, azimuth, the degree of polarization, and transmitted light power.

### 3. Results and Discussion

Using the optical scheme for digital polarization holography, shown in Figure 1, we inscribed polarization holographic gratings for two orientations of the sample—recording from the substrate side and from the azopolymer film side. In Figure 3, we present the kinetics of the DE for the  $\pm 1$  diffraction orders obtained during the recording of the PHG from the substrate side.

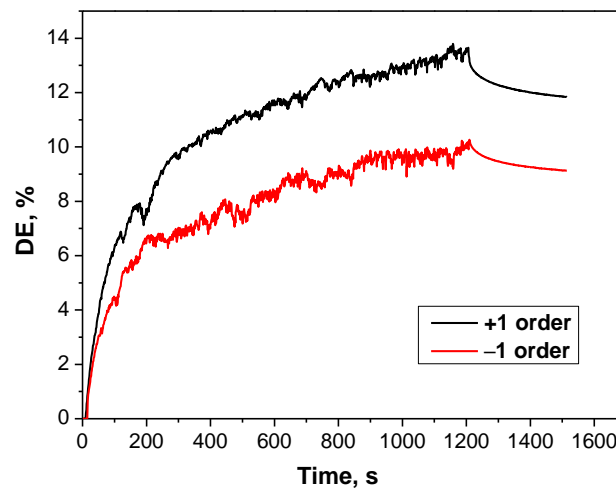


**Figure 3.** Kinetics of the DE in  $\pm 1$  diffracted orders in the case of recording PHGs from the substrate side.

As can be seen from the obtained DE kinetic curves, for recording from the substrate side, the maximum diffraction efficiency in the +1 order is approximately 14%, and, in the  $-1$  order, it is about 10%, i.e., the total diffraction efficiency is 24% at the end of the recording process.

To describe the diffraction from this type of grating, we can use the similarity with the polarization holographic gratings recorded with two coherent waves with orthogonal circular polarizations in the materials with photoinduced birefringence. Their properties are provided in detail in [15].

If two recording waves are incident on a photoanisotropic material (the PAZO polymer in our case) at small angles  $\theta$  and  $-\theta$  and they have equal intensities  $I$ , the Jones vector describing their interference field is as follows:

$$E = \sqrt{2I} \begin{vmatrix} \cos \delta \\ \sin \delta \end{vmatrix}, \tag{1}$$

where  $\delta = 2\pi \sin(\theta)x/\lambda$  is the phase shift between the recording waves,  $x$  is the distance along the horizontal axis, and  $\lambda$  is the wavelength. This interference field has no intensity modulation, and its polarization is linear with a gradually changing polarization direction. It induces anisotropy in the refractive index of the polymer, and the direction of the induced axis depends on  $\delta$ . For the Jones matrix, when describing the optical transmittance at  $\delta = 0$ , we can write the following:

$$T_{\delta=0} = \text{const.} \begin{vmatrix} \exp(i\Delta\varphi) & 0 \\ 0 & \exp(-i\Delta\varphi) \end{vmatrix}, \tag{2}$$

where  $\Delta\varphi = \pi\Delta nd/\lambda$ ;  $2\Delta n$  is the induced birefringence; and  $d$  is the thickness of the polymer layer. To obtain the Jones matrix of the entire grating, the matrix in Equation (2) must be rotated by an angle  $\delta = \delta(x)$ , or

$$T_G = R(\delta) T_G R(-\delta), \tag{3}$$

where

$$R(\delta) = \begin{vmatrix} \cos \delta & \sin \delta \\ -\sin \delta & \cos \delta \end{vmatrix} \tag{4}$$

is the rotation matrix. This results in the following:

$$T_G = \text{const.} \begin{vmatrix} \cos \Delta\varphi + i\sin \Delta\varphi \cos 2\delta & i\sin \Delta\varphi \sin 2\delta \\ i\sin \Delta\varphi \sin 2\delta & \cos \Delta\varphi - i\sin \Delta\varphi \cos 2\delta \end{vmatrix} \tag{5}$$

It can be easily seen that the recorded grating has only two orders of diffraction, +1 order and -1 order, and the waves diffracted in these orders are strongly dependent on the ellipticity of the probe beam; they are determined with the following matrices:

$$T_{+1} = \frac{1}{2} i \sin \left( \frac{\pi \Delta n d}{\lambda} \right) \begin{vmatrix} 1 & i \\ i & -1 \end{vmatrix} \exp(i2\delta) \tag{6}$$

and

$$T_{-1} = \frac{1}{2} i \sin \left( \frac{\pi \Delta n d}{\lambda} \right) \begin{vmatrix} 1 & -i \\ -i & -1 \end{vmatrix} \exp(-i2\delta) \tag{7}$$

Therefore, if the Jones vector of the reading beam for right/left elliptical polarization is

$$R = \begin{vmatrix} \cos \varepsilon \\ \pm i \sin \varepsilon \end{vmatrix}, \tag{8}$$

then the intensities of the two diffracted orders can be calculated as

$$I_{\pm 1} = \frac{1}{2} \sin^2 \left( \frac{\pi \Delta n d}{\lambda} \right) \cdot (1 \pm \sin 2\varepsilon), \tag{9}$$

where  $\varepsilon$  is the ellipticity angle of the probe beam.

In the case of our grating, recorded with light field polarization determined via the SLM, as shown in Figure 1, we have more than two diffracted orders (the higher orders having much smaller intensities), but we believe that the intensities of the  $\pm 1$  orders are given by analogical expressions. So, in Figure 4, we have plotted the curves

$I_{\pm 1} = C(1 \pm \sin 2\epsilon)$  with solid lines, where  $C$  is half the maximum value of the measured diffraction efficiency.

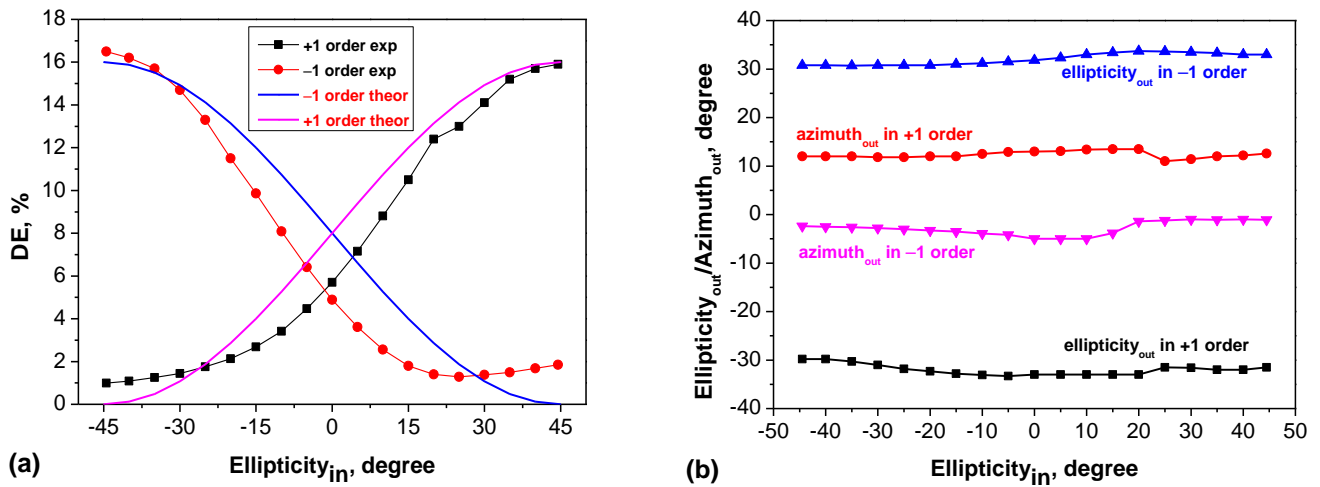


**Figure 4.** Dependencies of the diffraction efficiency (a), ellipticity, and azimuth (b) of  $\pm 1$  diffracted orders of the PHG on the angle of the ellipticity of the probe beam in the case of recording from the substrate side.

If we consider the experimentally determined DE vs. ellipticity dependence (Figure 4a), we can see that, when changing the input ellipticity from left circular polarization (LCP) to right circular polarization (RCP), a transfer of energy from  $-1$  to  $+1$  diffraction order is observed. The maximum DE value is around 17%. Hence, its behavior is very close to the theoretical model for grating recorded with two orthogonal (left and right) circular polarizations.

We should also note that there is no significant change (modulation) in the output ellipticity and output azimuth when changing the input ellipticity for both orders (Figure 4b). These properties are typical for polarization-selective gratings. The deviation between the theoretical calculation and experimental data can be explained with two effects as follows: (a) appearance of surface relief grating, even with small modulation, and (b) the fact that the continuous variation of the azimuth of the recording light field, which is assumed in the model, in our experiment is simulated by only four discrete azimuth values.

For comparison, for PHGs recorded from the azopolymer film side, a higher DE was achieved (Figure 5a), approximately 22% in the  $+1$  order and nearly 40% for the two diffracted orders. As known, this is due to the presence of a surface relief grating. This is also indicated by the much longer exposure time required for the SRG to form. On the other hand, however, the polarization properties of this grating have degraded (Figure 5b) due to the stronger influence of the surface relief grating.

In order to analyze the surface topography of both recorded gratings, we used an atomic force microscope (Asylum Research MFP-3D, Oxford Instruments, Abingdon, UK) supplied with standard silicon probes AC160TS-R3, operating at 300 kHz with a spring constant of 26 N/m. For better visualization of the features of the resulting surface relief, the measured area was set to  $20 \mu\text{m} \times 20 \mu\text{m}$ .

In Figure 6a, a relief amplitude of about 80 nm is observed, while, in Figure 6b, the height of the surface relief is of the order of 200 nm. This confirms the data already shown regarding the diffraction efficiency and polarization properties of the recorded PHGs in the two cases.

To characterize the volume anisotropic grating for the sample recorded through the substrate, we have used a polarization optical microscope operating in reflection mode (Zeta-20 Optical Microscope, Zeta Instruments, San Jose, CA, USA). The polarization pattern presented in Figure 7 was obtained with a 50x microscope objective, and the polarizer

and analyzer were oriented at  $90^\circ$ . As can be seen from the high contrast of the image, birefringence with significant modulation is induced in the sample during the recording process.

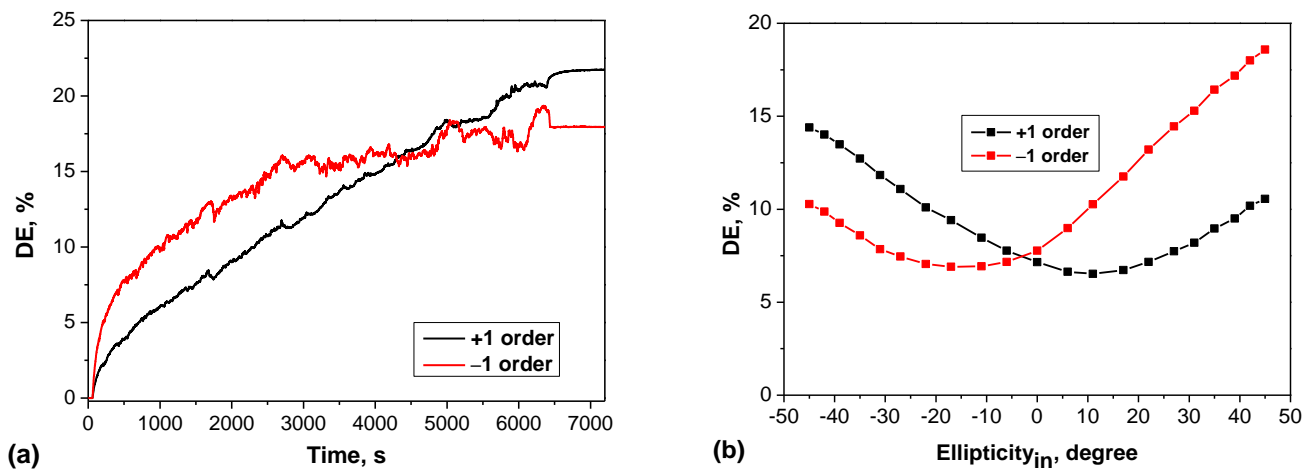


**Figure 5.** (a) Kinetics of the DE in  $\pm 1$  diffracted orders for PHGs recorded from the azopolymer film side; (b) dependency of the DE for  $\pm 1$  diffracted orders of the PHG on the ellipticity of the probe beam for PHGs recorded from the azopolymer film side.

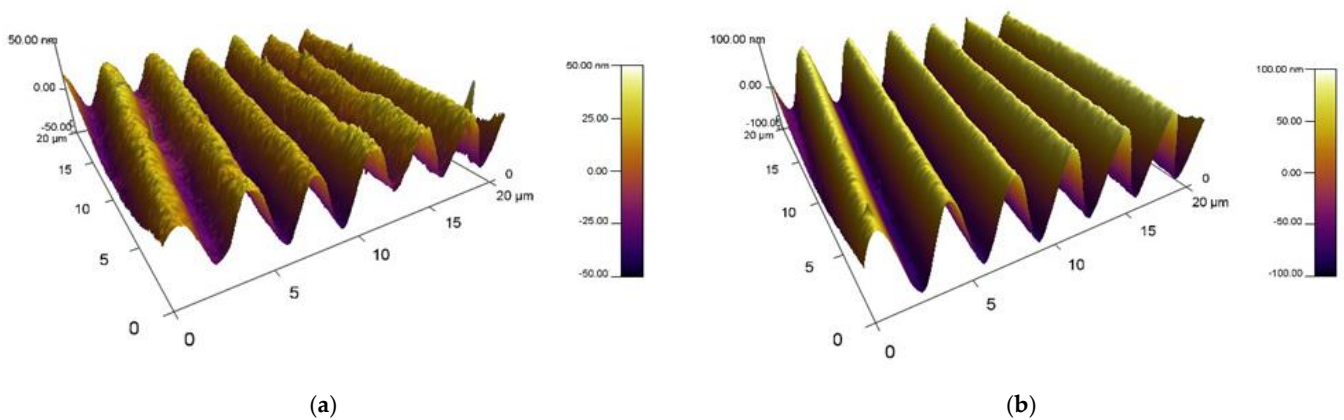


**Figure 6.** AFM images of the PHGs recorded from the substrate side (a) and from the azopolymer film side (b).

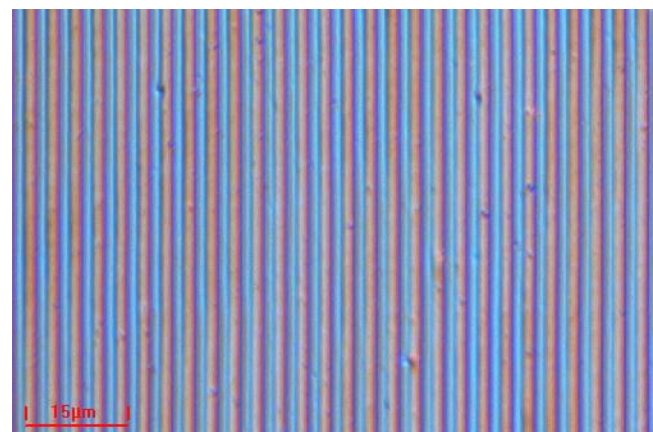


**Figure 7.** Polarization optical microscope images of the PHG recorded from the substrate side.

We should also comment on the photoanisotropic azopolymer material used in the present investigation. Most of the researchers working in the field of digital polarization holography use either proprietary photoalignment materials or azopolymers synthesized in their own laboratories, which makes it difficult to reproduce and verify the results reported. On the other hand, the azopolymer PAZO we used here is a well studied, easily accessible, and commercially available azopolymer which allows for the straightforward replication of the polarization gratings described in our work and for usage in a broad range of applications.

Finally, it is worth discussing the complex tradeoff between the grating area on the azopolymer film, the exposure time, the SLM pixel size, and the period of the recorded polarization holographic grating. Here, an interesting parallel can be made between our study and the results reported by Strobelt et al. [68]. In the optical scheme used by us, the lens system L1-L2 reduces the size of the SLM image by a ratio of 3.75:1 when projecting it on the film surface. In this way, relatively large gratings, with an area of about 6 mm<sup>2</sup>, can be inscribed with a single exposure. The exposure time, however, is large (of the order of minutes and even hours) due to the low intensity of the recording beam. On the other hand, in the optical scheme proposed in [68], a microscope objective is used, which reduces the projected image by about 140 times when compared to the SLM original dimensions. The size of the microgratings is 126 μm × 80 μm, which corresponds to an area of about 0.01 mm<sup>2</sup>. At the same time, this allows the reduction of the recording time to 5 s, while still being able to obtain a surface relief modulation of more than 300 nm.

We have chosen relatively a small reduction ratio of the lens system in order to obtain larger size gratings, so that their polarization properties can be reliably analyzed. This, however, imposes certain limitations on the grating resolution or the minimal grating period that can be reached, due to the finite pixel size, which is, in our case, 6.4 μm. Even in the case of a binary grating, the smallest grating period is two pixels, which corresponds to a 3.4 μm period on the film surface. To represent more faithfully the azimuth rotation pattern in the case of the interference of left and right circularly polarized beams, we have selected a four-pixel periodicity of the SLM gray levels, which are converted to four discrete azimuth values. Still, our results show that the polarization characteristics of this “simplified” grating are very close to those of an ideal grating recorded with continuous azimuth variation. At the same time, choosing only a four-pixel period on the SLM allows us to obtain a polarization grating with relatively high spatial frequency and, as a result, a large angle of diffraction. This is important for applications as polarization-selective DOEs as it enables more compact device implementation.

#### 4. Conclusions

Using a digital polarization holographic setup, we have inscribed and studied the polarization properties of polarization holographic gratings, recorded in a commercially available azopolymer PAZO, via irradiation either from the azopolymer film side or from the substrate side of the samples. Using a small reduction ratio of the lens system (3.75:1), we were able to record fairly large gratings with a single exposure, with an area of about 6 mm<sup>2</sup> and a relatively high spatial frequency. The phase modulation of each pixel of the SLM was converted via two quarter-wave plates to the azimuth rotation of a linearly polarized light field with a four-pixel periodicity, namely with consecutive azimuth values of 0°, 45°, 90°, and 135°. Our experimental data indicate that when the recording is performed from the substrate side of the sample, i.e., when the SRG amplitude is reduced, even with four-pixel period, we can obtain grating with polarization properties very similar to the model holographic grating, recorded with left and right circular polarizations. A possible application of this type of polarization grating is a polarization-selective DOE that acts as a circular polarization beam splitter, dividing the left and right circularly polarized components of the incident light into the −1 and +1 diffraction orders, respectively.

On the other hand, in the case of recording from the side of the azopolymer film, a higher diffraction efficiency and surface relief modulation are observed; however, the

polarization selectivity is degraded. In this case, the obtained surface micro- and nano-structures can be used for applications in biophysics and as sensors, or can be replicated on other, non-photosensitive layers. In general, SLM-generated polarization gratings recorded on thin film samples not only enable the realization of polarization-selective optical elements with spatial symmetry as gratings, lenses, etc., but also allow us to realize any kind of arbitrary wavefront optical structure as, for example, polarization encoded image that can then be used for security applications.

**Author Contributions:** Conceptualization, L.N. (Lian Nedelchev), L.N. (Ludmila Nikolova) and D.N.; validation, L.N. (Lian Nedelchev) and D.N.; formal analysis, N.B.-B. and K.H.; investigation, G.M., N.B.-B., B.I. and V.S.; writing—original draft preparation, N.B.-B. and L.N. (Ludmila Nikolova); writing—review and editing, L.N. (Lian Nedelchev) and D.N.; supervision, L.N. (Lian Nedelchev) and D.N.; funding acquisition, L.N. (Lian Nedelchev) and E.S. All authors have read and agreed to the published version of the manuscript.

**Funding:** This work was supported by the Institute of Information & Communications Technology Planning & Evaluation (IITP), grant No. 2019-0-00001. The authors are grateful for the funding from the European Union–NextGenerationEU, through the National Recovery and Resilience Plan of the Republic of Bulgaria, project BG-RRP-2.004-0002, “BiOrgaMCT”.

**Institutional Review Board Statement:** Not applicable.

**Informed Consent Statement:** Not applicable.

**Data Availability Statement:** All data generated or analyzed during this study are included in this published article.

**Acknowledgments:** The support provided by the Bulgarian National Science Fund (BNSF) through project KII-06-H38/15 is gratefully acknowledged. Research equipment of Distributed Research Infrastructure INFRAMAT, part of Bulgarian National Roadmap for Research Infrastructures, supported by Bulgarian Ministry of Education and Science, was used in this investigation.

**Conflicts of Interest:** The authors declare no conflicts of interest. The funders had no role in the design of the study; in the collection, analyses, or interpretation of data; in the writing of the manuscript; or in the decision to publish the results.

## References

1. Gabor, D. A New Microscopic Principle. *Nature* **1948**, *161*, 777–778. [[CrossRef](#)] [[PubMed](#)]
2. Leith, E.N.; Upatnieks, J. Reconstructed wavefronts and communication theory. *J. Opt. Soc. Am.* **1962**, *52*, 1123–1130. [[CrossRef](#)]
3. Goodman, J.W.; Lawrence, R. Digital image formation from electronically detected holograms. *Appl. Phys. Lett.* **1967**, *11*, 77–79. [[CrossRef](#)]
4. Hariharan, P. *Basics of Holography*; Cambridge University Press: Cambridge, UK, 2002. [[CrossRef](#)]
5. Azzam, R.M.A.; Bashara, N.M. *Ellipsometry and Polarized Light*; North-Holland Pub. Co.: Amsterdam, The Netherlands, 1977.
6. Born, M.; Wolf, E. *Principles of Optics: Electromagnetic Theory of Propagation, Interference, and Diffraction of Light*; Cambridge University Press: London, UK, 1999. [[CrossRef](#)]
7. Pancharatnam, S. Generalized theory of interference, and its applications. *Proc. Indian Acad. Sci.* **1956**, *44*, 247–262. [[CrossRef](#)]
8. Lohmann, A.W. Reconstruction of Vectorial Wavefronts. *Appl. Opt.* **1965**, *4*, 1667–1668. [[CrossRef](#)]
9. Kakichashvili, S.D. Method for phase polarization recording of holograms. *Sov. J. Quantum. Electron.* **1974**, *4*, 795. [[CrossRef](#)]
10. Todorov, T.; Nikolova, L.; Tomova, N. Polarization holography. 1: A new high-efficiency organic material with reversible photoinduced birefringence. *Appl. Opt.* **1984**, *23*, 4309–4312. [[CrossRef](#)] [[PubMed](#)]
11. Colomb, T.; Dahlgren, P.; Beghuin, D.; Cuhe, E.; Marquet, P.; Depeursinge, C. Polarization imaging by use of digital holography. *Appl. Opt.* **2002**, *41*, 27–37. [[CrossRef](#)] [[PubMed](#)]
12. Hong, Y.F.; Zang, J.L.; Liu, Y.; Fan, F.L.; Wu, A.A.; Shao, L.; Kang, G.G.; Tan, X.D. Review and prospect of polarization holography. *Chin. Opt.* **2017**, *10*, 588–602. [[CrossRef](#)]
13. Zhai, Y.; Cao, L.; Liu, Y.; Tan, X. A Review of Polarization-Sensitive Materials for Polarization Holography. *Materials* **2020**, *13*, 5562. [[CrossRef](#)]
14. Natansohn, A.; Rochon, P.; Gosselin, J.; Xie, S. Azo polymers for reversible optical storage. 1. Poly [4'-[[2-(acryloyloxy)ethyl]ethylamino]-4-nitroazobenzene]. *Macromolecules* **1992**, *25*, 2268–2273. [[CrossRef](#)]
15. Nikolova, L.; Ramanujam, P.S. *Polarization Holography*; Cambridge University Press: Cambridge, UK, 2009. [[CrossRef](#)]
16. Eich, M.; Wendorff, J.H.; Reck, B.D.; Ringsdorf, H.P. Reversible digital and holographic optical storage in polymeric liquid crystals. *Makromol. Chem. Rapid Commun.* **1987**, *8*, 59–63. [[CrossRef](#)]

17. Priimagi, A.; Shevchenko, A. Azopolymer-Based Micro- and Nanopatterning for Photonic Applications. *J. Polym. Sci. Part B Polym. Phys.* **2014**, *52*, 163–182. [[CrossRef](#)]
18. Nedelchev, L.; Mateev, G.; Nikolova, L.; Nazarova, D.; Ivanov, B.; Strijkova, V.; Stoykova, E.; Choi, K.; Park, J. In-line and off-axis polarization-selective holographic lenses recorded in azopolymer thin films via polarization holography and polarization multiplexing. *Appl. Opt.* **2022**, *62*, D1–D7. [[CrossRef](#)] [[PubMed](#)]
19. Wang, X. *Azo Polymers: Synthesis, Functions and Applications*; Springer: Berlin/Heidelberg, Germany, 2017. [[CrossRef](#)]
20. Nedelchev, L.; Mateev, G.; Strijkova, V.; Salgueiriño, V.; Schmool, D.S.; Berberova-Buhova, N.; Stoykova, E.; Nazarova, D. Tunable Polarization and Surface Relief Holographic Gratings in Azopolymer Nanocomposites with Incorporated Goethite ( $\alpha$ -FeOOH) Nanorods. *Photonics* **2021**, *8*, 306. [[CrossRef](#)]
21. Martínez-Ponce, G.; Solano, C.E.; Rodríguez-González, R.J.; Larios-López, L.; Navarro-Rodríguez, D.; Nikolova, L. All-optical switching using supramolecular chiral structures in azopolymers. *J. Opt. A Pure Appl. Opt.* **2008**, *10*, 115006. [[CrossRef](#)]
22. Blagoeva, B.; Nedelchev, L.; Nazarova, D.; Stoykova, E.; Park, J. Reversible supramolecular chiral structures induced in azopolymers by elliptically polarized light: Influence of the irradiation wavelength and intensity. *Appl. Opt.* **2021**, *61*, B147–B155. [[CrossRef](#)] [[PubMed](#)]
23. Natansohn, A.; Rochon, P. Photoinduced motions in azo-containing polymers. *Chem. Rev.* **2002**, *102*, 4139–4176. [[CrossRef](#)]
24. Rochon, P.; Batalla, E.; Natansohn, A. Optically induced surface gratings on an aromatic polymer films. *Appl. Phys. Lett.* **1995**, *66*, 136–138. [[CrossRef](#)]
25. Kim, D.; Li, L.; Kumar, J.; Tripathy, S.K. Laser-induced holographic surface relief gratings on nonlinear optical polymer films. *Appl. Phys. Lett.* **1995**, *66*, 1166–1168. [[CrossRef](#)]
26. Holme, N.C.; Nikolova, L.; Ramanujam, P.S.; Hvilsted, S. An analysis of the anisotropic and topographic gratings in a side-chain liquid crystalline azobenzene polyester. *Appl. Phys. Lett.* **1997**, *70*, 1518–1520. [[CrossRef](#)]
27. Cipparrone, G.; Pagliusi, P.; Provenzano, C.; Shibaev, V.P. Polarization holographic recording in amorphous polymer with photoinduced linear and circular birefringence. *J. Phys. Chem. B* **2010**, *114*, 8900–8904. [[CrossRef](#)] [[PubMed](#)]
28. Martínez-Ponce, G. Mueller imaging polarimetry of holographic polarization gratings inscribed in azopolymer films. *Opt. Express* **2016**, *24*, 21364–21377. [[CrossRef](#)] [[PubMed](#)]
29. Berberova-Buhova, N.; Nedelchev, L.; Mateev, G.; Stoykova, E.; Strijkova, V.; Nazarova, D. Influence of the size of Au nanoparticles on the photoinduced birefringence and diffraction efficiency of polarization holographic gratings in thin films of azopolymer nanocomposites. *Opt. Mat.* **2021**, *121*, 111560. [[CrossRef](#)]
30. Nair, S.; Escobedo, C.; Sabat, R.G. Crossed Surface Relief Gratings as Nanoplasmonic Biosensors. *ACS Sens.* **2017**, *2*, 379–385. [[CrossRef](#)] [[PubMed](#)]
31. Kryshenik, V.M.; Azhniuk, Y.M.; Kovtunenkov, V.S. All-optical patterning in azobenzene polymers and amorphous chalcogenides. *J. Non-Cryst. Solids* **2019**, *512*, 112–131. [[CrossRef](#)]
32. Lin, Y.; Xu, H.; Shi, R.; Lu, L.; Zhang, S.; Li, D. Enhanced diffraction efficiency with angular selectivity by inserting an optical interlayer into a diffractive waveguide for augmented reality displays. *Opt. Express* **2022**, *30*, 31244–31255. [[CrossRef](#)] [[PubMed](#)]
33. Mateev, G.; Nedelchev, L.; Nikolova, L.; Ivanov, B.; Strijkova, V.; Stoykova, E.; Choi, K.; Park, J.; Nazarova, D. Two-Dimensional Polarization Holographic Gratings in Azopolymer Thin Films: Polarization Properties in the Presence or Absence of Surface Relief. *Photonics* **2023**, *10*, 728. [[CrossRef](#)]
34. Nazarova, D.; Nedelchev, L.; Berberova-Buhova, N.; Mateev, G. Nanocomposite Photoanisotropic Materials for Applications in Polarization Holography and Photonics. *Nanomaterials* **2023**, *13*, 2946. [[CrossRef](#)]
35. Ferreira, Q.; Gomes, P.; Raposo, M.; Giacometti, J.; Oliveira, O.; Ribeiro, P. Influence of ionic interactions on the photoinduced birefringence of poly [1-[4-(3-Carboxy-4-hydroxyphenylazo) benzene sulfonamido]-1,2-ethanediyl, sodium salt] films. *J. Nanosci. Nanotechnol.* **2007**, *7*, 2659–2666. [[CrossRef](#)]
36. Madruga, C.; Filho, P.; Andrade, M.; Gonçalves, M.; Raposo, M.; Ribeiro, P. Birefringence dynamics of poly{1-[4-(3-carboxy-4-hydroxyphenylazo) benzenesulfonamido]-1,2-ethanediyl, sodium salt} cast films. *Thin Solid Films* **2011**, *519*, 8191–8196. [[CrossRef](#)]
37. Nedelchev, L.; Ivanov, D.; Berberova, N.; Strijkova, V.; Nazarova, D. Polarization holographic gratings with high diffraction efficiency recorded in azopolymer PAZO. *Opt. Quantum Electron.* **2018**, *50*, 212. [[CrossRef](#)]
38. Blagoeva, B.; Nedelchev, L.; Mateev, G.; Stoykova, E.; Nazarova, D. Diffraction efficiency of polarization holographic gratings recorded in azopolymer thin films coated using different solvents. In *Photosensitive Materials and Their Applications*; SPIE: Bellingham, WA, USA, 2020; Volume 11367, pp. 190–195. [[CrossRef](#)]
39. Falcione, R.; Roldan, M.V.; Pellegrini, N.; Goyanes, S.; Ledesma, S.A.; Capeluto, M.G. Increase of SRG modulation depth in azopolymers-nanoparticles hybrid materials. *Opt. Mater.* **2021**, *115*, 111015. [[CrossRef](#)]
40. Stoilova, A.; Mateev, G.; Nazarova, D.; Nedelchev, L.; Stoykova, E.; Blagoeva, B.; Berberova, N.; Georgieva, S.; Todorov, P. Polarization holographic gratings in PAZO polymer films doped with particles of biometals. *J. Photochem. Photobiol. A Chem.* **2021**, *411*, 113196. [[CrossRef](#)]
41. Takeda, M.; Ina, H.; Kobayashi, S. Fourier-Transform Method of Fringe- Pattern Analysis for Computer-Based Topography and Interferometry. *J. Opt. Soc. Am.* **1982**, *72*, 156–160. [[CrossRef](#)]
42. Kim, M.K. *Digital Holographic Microscopy: Principles, Techniques, and Applications*; Springer: New York, NY, USA, 2011. [[CrossRef](#)]
43. Schnars, U.; Falldorf, C.; Watson, J.; Jueptner, W. *Digital Holography and Wavefront Sensing: Principles, Techniques and Applications*; Springer: Berlin/Heidelberg, Germany, 2014.

44. Kostuk, R.K. *Holography: Principles and Applications*; CRC Press: Boca Raton, FL, USA, 2019.
45. Shan, M.; Liu, L.; Zhong, Z.; Liu, B.; Zhang, Y. Direct phase retrieval for simultaneous dual-wavelength off-axis digital holography. *Opt. Lasers Eng.* **2019**, *121*, 246–251. [[CrossRef](#)]
46. Tahara, T.; Ito, T.; Ichihashi, Y.; Oi, R. Single-shot incoherent color digital holographic microscopy system with static polarization-sensitive optical elements. *J. Opt.* **2020**, *22*, 105702. [[CrossRef](#)]
47. Liu, L.; Shan, M.; Zhong, Z.; Liu, B.; Luan, G.; Diao, M.; Zhang, Y. Simultaneous dual-wavelength off-axis flipping digital holography. *Opt. Lett.* **2017**, *42*, 4331–4334. [[CrossRef](#)] [[PubMed](#)]
48. Tahara, T.; Quan, X.; Otani, R.; Takaki, Y.; Matoba, O. Digital holography and its multidimensional imaging applications: A review. *Microscopy* **2018**, *67*, 55–67. [[CrossRef](#)]
49. Kim, H.; Kim, D.H.; Lee, Y. Encryption of digital hologram of 3-D object by virtual optics. *Opt. Express* **2004**, *12*, 4912–4921. [[CrossRef](#)]
50. Di, H.; Zheng, K.; Zhang, X.; Lam, E.Y.; Kim, T.; Kim, Y.S.; Poon, T.; Zhou, C. Multiple-image encryption by compressive holography. *Appl. Opt.* **2012**, *51*, 1000–1009. [[CrossRef](#)] [[PubMed](#)]
51. Javidi, B.; Kim, D. Three-dimensional-object recognition by use of single-exposure on-axis digital holography. *Opt. Lett.* **2005**, *30*, 236–238. [[CrossRef](#)] [[PubMed](#)]
52. Stoykova, E.; Alatan, A.A.; Benzie, P.; Grammalidis, N.; Malassiotis, S.; Ostermann, J.; Zabulis, X. 3-D time-varying scene capture technologies—A survey. *IEEE Transactions on Circuits and Systems for Video Technology* **2007**, *17*, 1568–1586. [[CrossRef](#)]
53. Liu, J.-P.; Tahara, T.; Hayasaki, Y.; Poon, T.-C. Incoherent Digital Holography: A Review. *Appl. Sci.* **2018**, *8*, 143. [[CrossRef](#)]
54. Tiwari, V.S.; Bisht, N. *Spatial Light Modulators and Their Applications in Polarization Holography*; IntechOpen: London, UK, 2023. [[CrossRef](#)]
55. Yang, Y.Q.; Forbes, A.; Cao, L.C. A review of liquid crystal spatial light modulators: Devices and applications. *Opto-Electron. Sci.* **2023**, *2*, 230026. [[CrossRef](#)]
56. Chen, H.C.; Cheng, C. Holographic Optical Tweezers: Techniques and Biomedical Applications. *Appl. Sci.* **2022**, *12*, 10244. [[CrossRef](#)]
57. Kuang, Z.; Li, J.; Edwardson, S.; Perrie, W.; Liu, D.; Dearden, G. Ultrafast laser beam shaping for material processing at imaging plane by geometric masks using a spatial light modulator. *Opt. Lasers Eng.* **2015**, *70*, 1–5. [[CrossRef](#)]
58. Vijayakumar, A.; Kashter, Y.; Kelner, R.; Rosen, J. Coded aperture correlation holography—a new type of incoherent digital holograms. *Opt. Express* **2016**, *24*, 12430–12441. [[CrossRef](#)] [[PubMed](#)]
59. Davis, J.A.; McNamara, D.E.; Cottrell, D.M.; Sonehara, T. Two-dimensional polarization encoding with a phase-only liquid-crystal spatial light modulator. *Appl. Opt.* **2000**, *39*, 1549–1554. [[CrossRef](#)]
60. Singh, R.K. Digital Polarization Holography: Challenges and Opportunities. *Eng. Proc.* **2023**, *34*, 10. [[CrossRef](#)]
61. De Sio, L.; Roberts, D.E.; Liao, Z.; Nersisyan, S.R.; Uskova, O.; Wickboldt, L.; Tabiryan, N.V.; Steeves, D.M.; Kimball, B.R. Digital polarization holography advancing geometrical phase optics. *Opt. Express* **2016**, *24*, 18297–18306.
62. Shen, Y.; Wang, X.; Xie, Z.; Min, C.; Fu, X.; Liu, Q.; Gong, M.; Yuan, X. Optical vortices 30 years on: OAM manipulation from topological charge to multiple singularities. *Light Sci. Appl.* **2019**, *8*, 90. [[CrossRef](#)] [[PubMed](#)]
63. Fernández, R.; Gallego, S.; Márquez, A.; Neipp, C.; Calzado, E.M.; Francés, J.; Morales-Vidal, M.; Beléndez, A. Complex Diffractive Optical Elements Stored in Photopolymers. *Polymers* **2019**, *11*, 1920. [[CrossRef](#)] [[PubMed](#)]
64. Cazac, V.; Achimova, E.; Abashkin, V.; Prisacar, A.; Loshmanshii, C.; Meshalkin, A.; Egiazarian, K. Polarization holographic recording of vortex diffractive optical elements on azopolymer thin films and 3D analysis via phase-shifting digital holographic microscopy. *Opt. Express* **2021**, *29*, 9217–9230. [[CrossRef](#)] [[PubMed](#)]
65. Tabiryan, N.V.; Nersisyan, S.R.; Xianyu, H.; Serabyn, E. Fabricating vector vortex waveplates for coronagraphy. In Proceedings of the IEEE Aerospace Conference, Big Sky, MT, USA, 3–10 March 2012; pp. 1–12. [[CrossRef](#)]
66. Gong, L.; Ren, Y.; Liu, W.; Wang, M.; Zhong, M.; Wang, Z.; Li, Y. Generation of cylindrically polarized vector vortex beams with digital micromirror device. *J. Appl. Phys.* **2014**, *116*, 183105. [[CrossRef](#)]
67. Tabiryan, N.V.; Serak, S.V.; Roberts, D.E.; Steeves, D.M.; Kimball, B.R. Thin waveplate lenses of switchable focal length—New generation in optics. *Opt. Express* **2015**, *23*, 25783–25794. [[CrossRef](#)] [[PubMed](#)]
68. Strobelt, J.; Stolz, D.; Leven, M.; Soelen, M.V.; Kurlandski, L.; Abourahma, H.; McGee, D.J. Optical microstructure fabrication using structured polarized illumination. *Opt. Express* **2022**, *30*, 7308–7318. [[CrossRef](#)]
69. Porfirev, A.; Khonina, S.; Ivliev, N.; Meshalkin, A.; Achimova, E.; Forbes, A. Writing and reading with the longitudinal component of light using carbazole-containing azopolymer thin films. *Sci. Rep.* **2022**, *12*, 3477. [[CrossRef](#)]

**Disclaimer/Publisher’s Note:** The statements, opinions and data contained in all publications are solely those of the individual author(s) and contributor(s) and not of MDPI and/or the editor(s). MDPI and/or the editor(s) disclaim responsibility for any injury to people or property resulting from any ideas, methods, instructions or products referred to in the content.